Available online at www.sciencedirect.com
ScienceDirect
Fuel 87 (2008) 2551–2562
FUEL
www.fuelfirst.com

Deactivation of WNiPd/$TiO_2Al_2O_3$ catalyst during the upgrading of LCO

Roberto Galiasso Tailleur *

Simón Bolívar University, Satenejas, Baruta, Edo. Miranda, Venezuela

Received 13 September 2007; accepted 31 January 2008
Available online 27 February 2008

Abstract

The deactivation of a novel catalyst during the production of a high-quality low-emission diesel component has been studied experimentally in a hydrotreating microplant. This process is compared with a commercial operation that used a conventional HDT catalyst. Catalysts were tested by incrementing temperature as a function of cycle length to keep the sulfur constant in the product, maintaining all other operating conditions constant. Spent catalysts were characterized using solid ^{13}CNMR and XPS spectroscopy, pyridine adsorption, GC–MS of the coke extracted, and chemical analysis. Effective pore diffusivity was measured with pentane, and the catalyst activity and selectivity were measured with LCO and probe molecules to verify naphthenic ring opening capability. An important decline in hydrogenation and ring opening activity was detected along the cycle length due to acid site deactivation. The deactivation is attributed to LCO poly-aromatics adsorption on a particular type of acid site. A commercially deactivated HDT catalyst that operated with LCO presents a similar type of coke to that of the pilot plant.

Keywords: Hydrotreating; LCO hydrogenation; Lewis acid sites; Coke; NO_x and PM emissions

1. Introduction

The upgrading of LCO (light catalytic oil) using high-pressure hydrotreating (HDT) commercial units to produce a low-sulfur high-cetane diesel is a growing area of interest. Babich and Moulijn [1] and this author [2], among others, have performed analysis of different options for revamping existing HDT units to produce a high-quality diesel using such low-value refinery streams as LCO (light FCC gas oil) and LCGO (light coker gas oil). The key point in any possible scenario is catalyst deactivation, as the optimum hydrotreating cycle length depends on the composition of feedstock and its effect on some active centers on the catalyst surface. In particular, when cracked material is used as feedstock, the important issue is the transformation of the high-molecular-weight alkyl-poly-aromatics into *n*- and isoparaffins with high volumetric yields and moderate hydrogen consumption to improve cetane number and reduce emissions.

The standard commercial practice is to blend LCO with other light gas oils and to perform a high-pressure hydrotreatment on the combination. The economy of this process is strongly dependent upon hydrogen availability, type of unit, and quality and proportion of LCO incorporated in the feed. With more than 50% of LCO in the hydrotreating feed, a very low space velocity is required to obtain 15 ppm of sulfur and 42 cetane number [3] Considerable attention has been devoted in recent years to the development of new catalysts and processes for LCO upgrading, with particular emphasis on deep sulfur removal and aromatic saturation [4]. However, their analysis of the worldwide refinery industry indicated that some refineries still use a limited amount of LCO (less than 15% by weight) in the high-pressure hydrotreating units, producing 500 ppm sulfur diesel. At least in two of Gulf Coast refineries a notable

* Address: Department of Chemical Engineering, Texas A&M University, College Station, TX 77843, USA. Tel.: +1 979 218 1903; fax: +1 979 845 6446.
E-mail address: reg2005@chemail.tamu.edu

0016-2361/$ - see front matter © 2008 Elsevier Ltd. All rights reserved.
doi:10.1016/j.fuel.2008.01.025

phenomenon of catalyst deactivation and bed plugging was observed. These HDT units were using conventional last-generation catalysts that achieve only one year of operation at most. There is a high economic incentive to increase both the LCO and the cycle length.

Recently, a new catalyst to treat LCO based on WNiPd/$TiO_2Al_2O_3$ was developed [5]. This catalyst is able to reduce sulfur to very low levels and to improve the cetane number via aromatics hydrogenation and naphthenic ring opening. A previous study [6] showed that this catalyst had 30% higher hydrogenating and denitrogenating capabilities and 15% lower desulfurization activities than a Ni–Mo/Al_2O_3 commercial HDT catalyst. The main advantage of the new catalyst is its higher (15%) ability to carry out naphthenic ring opening reactions and its acid center stability. Deactivation of this type of catalyst occurs by adsorption of the coke precursor on the metal and acid sites. The acid strength distribution in the new catalyst – amorphous base-type structure – is broader than in zeolitic type ones, according to the pyridine thermo-desorption studies [5]. The adsorption energy of the heavy aromatic follows the acid distribution function, and in some of the strongest acid sites, the adsorbed material suffers dehydrogenation, cracking, and polymerization reactions that generate the coke precursors. In other weaker acid sites, the same molecules can follow other reactions, such as isomerization, cyclization, and ring opening, and the product can desorb from them.

The LCO used in this study boils in the diesel range. It contains a high percentage of aromatics (~60%) and sulfur (1.23%), and it has an extremely low cetane number. It is composed of 15% of mono-ring aromatics, 35% of di-ring aromatics, and 8% by weight of tri-ring aromatics. The material was produced in an HDS–FCC complex at the refinery using highly naphthenic vacuum gas oil, and it can be used as a diesel component only if it is deeply hydrotreated and most of the aromatics (80%) converted into paraffins. In a previous paper, Galiasso Tailleur [7] showed that diesel engine emissions can progressively be reduced by increasing the hydrotreatment severity to raise the cetane number of the LCO above 42, and to deeply reduce diaromatics and naphtheno-aromatics compounds content. Santana et al. [8], among others, evaluated different strategies for cetane number improvement via hydrogenation of aromatics. The poly-aromatics hydrogenation and ring opening reaction has been studied recently by many authors (cf. Refs. [9,10] and by this researcher [11]).

The hydrotreating catalysts used for middle distillates upgrading are deactivated by coke. The characterization of the carbonaceous deposits on reforming and isomerization and dehydrogenation catalysts was studied by several authors [12–15]. These authors, among others, performed fundamental studies by building coke using precursor molecules at different operating conditions and regenerating them by oxygen. Other researchers studied the hydrotreating catalyst deactivation [16–17]. They developed different methodologies for characterization of spent catalysts. In addition, a few studies have been done on catalyst deactivation of the ring opening function [18–19]. Despite results from these studies, scarce information is available about how affects coke the hydrogenation and ring opening reactions and how the cycle length can be optimized during the upgrading of LCO into a low-emission diesel fuel.

This paper focuses on the study of the WNiPd/$TiO_2Al_2O_3$ catalyst deactivation that occurs during the processing of LCO in a medium high-pressure HDT unit. It will concentrate on aromatic hydrogenation and ring opening reaction, as well as on evaluating the impact of deactivation in diesel engine emission. The performance of the catalyst deactivated in a microplant during the processing of 100% LCO-feed was study and compare to those obtained with a commercially deactivated catalyst that operated with 15% of LCO-feed. Although some characterization the coke deposit will be presented here, complementary information is under preparation to be published soon.

2. Experimental

2.1. Catalyst

The $TiO_2Al_2O_3$ support was prepared in the laboratory by a controlled co-precipitation of aluminum and titanium hydroxides. It was dried at 120 °C and calcinated at 450 °C in air. Pellets of 1 mm diameter and 1 mm length were prepared using a controlled high-pressure extruder machine. The two-step incipient wetness impregnation process consisted in using first an aqueous solutions of tungsten salt, then another of nickel and palladium salt. After impregnation, the solid was dried in air and calcinated at 550 °C. Three identical samples of the catalyst were installed in one fixed-bed microreactor and presulfided in situ. (See in Ref. [5] details about catalyst formulation and characterization.) These samples are used to process 100% of LCO at standard HDT conditions during 1, 4, and 10 weeks on stream to produce 50 ppm sulfur content products. At the end of the run, three deactivated samples were designated Spent 1, 2, and 3. A fourth sample of catalyst was previously used to treat straight run gas oil for three months at constant sulfur in the product.

Four samples of deactivated catalyst, with unknown composition, were obtained from the commercial plant at end-of-run (EOR) operating for one year using 15% of LCO in the feed. The four samples were mixed together, and the mixture designated Commercial. It is important to mention that plant shutdown procedures and download of catalyst has been previously used on more than 30 occasions for isomerization, reforming, hydrocracking, and hydrotreating catalyst withdrawal from commercial and pilot plant units during the last 17 years. The methodology controls the adsorbed hydrocarbons in the spent samples and preserves the reduced state of the metals.

The catalysts were washed in xylene for 24 h and dried in nitrogen to constant weight. Then samples at the laboratory were all manipulated under inert atmosphere in a vac-

uum chamber to avoid catalyst reoxidation. The solids were analyzed using the following techniques.

2.1.1. Physical method

Surface, pore volume, and average pore diameter, were measured using standard nitrogen adsorption (Micromeritics 250) and mercury porosimetry methods. A shallow-bed string reactor was used to measure the effective diffusivity employing a technique developed in the 1990 by the author [20]. There, seven particles of equal size were installed in the parallel channel and heated to the operating temperature (80 °C). Then the inert gas (He) was flowed at 2 cm^3/s until the pressure and temperature in the system were constant. The MS detector that measured the pentane inlet and outlet concentrations was calibrated to have a linear response in the range of concentration selected for the test. Then, a pulse of pentane was injected in the chamber, and changes in concentration output as a function of time were measured with fresh and spent catalyst to determine their macro, and meso–micro effective diffusivity.

2.1.2. Chemical characterization

Total metal analysis was performed using atomic absorption spectroscopy (Varian Techtron analyzer). C, H, N analysis were performed using a LECO (D5373) carbon analyzer; and sulfur by XRF (D1757). Metals were reported in wt% (bulk) of total metal in the support (W, Ni, or Ti on (Ti + Al) support). Total carbon, sulfur and hydrogen were reported in wt%.

2.1.3. Solid ^{13}CNMR spectra

The analysis of the carbon deposited on solids was performed using a Varian spectrometer operating at a frequency of 50.576 MHz with cross-polarization using adamantine as reference. The technique allowed detection of the type of carbon present on the surface. Aliphatic- and aromatic-type coke signals were recorded and integrated, and their relative amount calculated for further analysis.

2.1.4. CH_2Cl_2 extraction and GC–MS analysis

Deactivated catalyst samples, after being washed with xylene, were extracted in a column packed with the powder of the catalyst by elution with CH_2Cl_2 The elute organic material was concentrated by evaporation and then injected in a GC–MS system (HP 5890 Series II, HP-5 column with internal diameter 0.28 mm, 20 m length, with inner surface coated by methylsiloxane, HP 5972 mass spectrometer (HP-1MS column with a 0.28 mm internal diameter and 20 m length with the inner surface coated by methylsiloxane). Two 1 μdm^3 samples were injected for each catalyst fuel product. The whole spectrum was used as fingerprints to characterize soluble coke in CH_2Cl_2 (but insoluble in xylene). The 70% of peaks were identified using pure compounds and an MS library. The elemental analysis of the insoluble coke remaining on the surface was performed by dissolution of the inorganic matrix with fluorhydric acid, washing the remaining solid with water and ether, drying in nitrogen and performing the C, H, N analysis by LECO apparatus and S by X-ray fluorescence.

2.1.5. Pyridine TPD

Pyridine thermal desorption analysis was used to characterize the total acidity strength on catalysts as a function of time on stream: fresh, start of run (1 week on stream), 4 weeks, and 10 weeks on stream. A McBain microbalance with 1 mg of sample (thin layer) that can be transferred to specially designed IR cells was employed. The catalysts were pretreated with argon (3 dm^3/min) until achieving a constant weight using a program of 10 °C/min to increment the temperature from 30 °C to 200 °C or 300 °C. During this time, the weight losses were recorded. After that, the temperature was kept constant at 200 °C or 300 °C for 2 h and then cooled at a rate of 10 °C/min. A stream containing pyridine (0.001 molar) diluted in argon was passed through the catalyst at room temperature (30 °C) for 2 h. After that, pure argon was flowed at the same temperature for another 2 h. The catalyst sample was then characterized by FTIR spectroscopy (main bands: Lewis at 1445 cm^{-1}; Brönsted at 1540 cm^{-1}). Absorption intensities were calibrated using an internal standard and compared with those of fresh catalyst. Other samples of the same catalyst were used to adsorb pyridine (at the same operating conditions), but the solids after adsorption of pyridine, were heated in argon using a ramp of 6 °C/min, and the remaining amount of pyridine at 200 °C and 300 °C were measured and reported in mini-mol of pyridine per gram of solid. This analysis gives the total acidity (weight) and the ratio of strong to weak acid sites. The number of strong acid sites was calculated using the mol of pyridine retained at 300 °C (TPD), and the weak acid site by the mol retained at 200 °C minus those at 300 °C.

2.1.6. XPS

The XPS equipment was a Bruker 300 apparatus (Al cathode), that uses Al Kα 1486.6 eV, and with 200 W of power. For peak area measurements, a Shirley-type integral background was used [21]. When multiple components were present under a given XPS envelope, a non-linear least-square-curve fitting routine was implemented (Levenberg–Marquardt damping method). All peaks were fitted using a Voight function with 20% Lorentzian character. Curve fitting of the W4f region (42–32 eV) – complicated by the presence of Ti3p, the W "satellite" peaks, and the high carbon background – was carried out according to the methodology described by Galiasso and Prada [6]. The XPS parameters (peak position, peak width) relative to W^{+4} were obtained by curve fitting the spectra of the oxide samples. These parameters were kept constant when fitting the spectra of sulfide specimens. The parameters for the "sulfide" species were obtained by curve fitting the sample sulfide at 375 °C and allowing the peak position and its FWHM to relax into their local minima. The results were reported as exposed $I_W/(I_{Ti} + I_{Al})$ and $I_{Ti}/(I_{Ti} + I_{Al})$.

The dispersion was analyzed using different angles of beam incidence on the sample to check the coke attenuation of the signals.

2.2. Feed and product characterization

2.2.1. Analysis of the feedstock and HDT products

The fresh feed (LCO) and products were fractionated in three cuts (180–220 °C, 220–300 °C, 300–360 °C), each of which was analyzed using programmed-temperature GC techniques coupled with a low-intensity mass spectrometry method. In parallel, a preparative HPLC was also performed on each cut using a hexane carrier and an ultraviolet detector. The fractions were analyzed using a LECO elemental analyzer; ^{1}HNMR spectroscopy (Varian 400-MHz spectrometer, 10 mm broadband probe); alumina percolation method (using tetrahydrofuran as solvent); and mainly using high-resolution mass spectrometry (HRMS, Philips 2341). To integrate all this information, a computerized reconciliation procedure was used to fit the analysis of the full-range (180–360 °C) LCO with those results obtained, cut by cut. Using the described in-house-developed analysis, we were able to discriminate families of aromatics, naphthenes, and paraffins, and, in particular, track the production and transfer from one cut to another of alkyl-mono-ring-aromatics and alkyl-mono-ring-naphthenes. The cetane number was determined by using the D613 ASTM method.

2.2.2. Diesel engine test

The specialized literature (cf. EPA report [22]) indicates some correlation between exhaust gas emissions and cetane number in former heavy-duty diesel engines. More recently, we confirmed the effect of aromatics on 2002 EURO III heavy-duty diesel engine emissions. Here the NO_x (nitrogen oxide) and PM (particulate) emissions were measured in a high-speed Mercedes-Benz LD (2002), direct-injection engine operating at 2000 rpm, 350 kW power, 1.364 MPa break mean effective pressure (BMEP), 1630 N m torque, and without EGR (exhaust gas recirculation) and post-treatment. To determine NO_x and PM, a micro-tunnel device coupled with online micro-filter and IR analyzer were used. The heat-released curve was analyzed at stationary conditions and operating in transient mode (EURO III-type of driving cycle). Three samples of LCO hydrotreated to 50 ppm of sulfur with Spent 1, 2 or 3 catalyst were blended with a 48-ppm-sulfur, 46-cetane-number SRGO in a proportion 25–75 wt% to produce a low-sulfur diesel for engine testing. The emission results are compared to those of an end-of-run commercial diesel.

2.3. Chemical reaction

2.3.1. Microplant long run tests

The microplant has a conventional isothermal downflow fixed-bed reactor [5]. It was operated at temperatures from 350 °C to 378 °C, and 0.2 h^{-1} (LHSV), 4 (molar) of H_2/HC ratio, and 12.5 MPa of total pressure. 50 g of WNiPd on $TiO_2Al_2O_3$ catalyst was loaded in the reactor diluted with 50% of inert material, which had 1-mm particle diameter, to improve the reactor fluid-dynamics (see the methodology in [23], among others). The catalyst was pre-activated in situ with straight run light gas oil spiked with 1% of CS_2 at 300 °C for 6 h. Then the microreactor was started up with LCO and operated continuously for 1 week, or 4 weeks, or 10 weeks on stream, generating the catalysts and products called Spent 1, 2, and 3, respectively. Duplicate samples of hydrotreated LCO were taken daily, and mass balance was performed to check the operation. Having achieved the period on stream, the catalyst was cooled down to 200 °C, washed with xylene for a half day, and then dried with nitrogen at 200 °C for another half day. After washing, the deactivated catalyst was ready to be tested with synthetic feedstock. The procedure for the three samples of spent catalysts was identical.

2.3.2. Test with synthetic feed (probe molecules)

The spent catalysts were tested using a blend of 30% naphthalene, 10% tetralin, and 1.5 wt% of sulfur as dibenzothiophene in hexadecane. The temperature was 340, 348, or 363 °C; and the other operating conditions were: 0.8 h^{-1} of LHSV, 4 of H_2/HC molar ratio, and 12.5 MPa of total pressure. The temperature was adjusted to reach the same constant DBT conversion (50 ppm of sulfur) for either Spent 1, 2 or 3 catalysts. Finally, the catalysts were washed by continuous pumping of xylene at 200 °C for 24 h, dried in nitrogen for another half day (120 °C) and discharged in a dried-inert chamber. The three samples of spent catalyst were characterized together, along with the one from a commercial plant.

3. Results and discussion

3.1. Catalyst characterization

The main catalyst contained W, Ni, and Pd as the metal active phase. The support is based on $TiO_2Al_2O_3$, a low-acidity type of active support. The analysis of physical properties indicates that the solid has a high-surface, medium-pore-volume structure with a large contribution of interconnected mesopores and an average pore diameter of 12 nm (Table 1). The chemical composition of the catalyst is: 4.2% NiO, 12.5% WO_3, 0.2% PdO, 12% by weight of TiO_2; the complement is Al_2O_3. After pre-activation (sulfiding), the fresh catalyst contains 5.4% weight of sulfur and less than 0.1% of carbon (Table 1).

It can be observed in Table 1 that at the start of run (SOR) after 1 week on stream, the catalyst contained 5.4% of carbon, and had lost 40% of its surface, 15% of pore volume, and 48% of micropores volume compared with the fresh catalyst. Then, after the 4th and 10th weeks (end-of-run of sustained operation), the physical properties of the spent catalyst continued to decline, showing additional losses in surface area and pore volume, while the car-

Table 1
Fresh and spent catalysts properties

Catalysts	Fresh	Spent 1	Spent 2	Spent 3	Commercial
Surface (m^2/g)	245	145	132	112	–
Pore volume (cm^3/g)	0.52	0.44	0.4	0.38	0.28
Micropores volume (cm^3/g)	0.22	0.1	0.08	0.07	0.08
Average pore diameter (nm)	12	14	15	16	12
Adsorbed pyridine (mmol/g) 200 °C/300 °C	0.28/0.2	0.14/0.08	0.10/0.05	0.03/0.01	0.014/0.01
D_{effMac}/D_{effMic} (cm^2/s^*10^4)	1.2/0.3	0.77/0.1	0.69/0.08	0.68/0.09	0.55/0.08
Sulfur (wt%)	5.4	6.1	6.2	6.1	6.2
Carbon (total) (wt%)	0.1	5.4.	5.8	6.2	6.0
CH_2Cl_2 soluble coke (wt%)	–	0.28	0.19	0.14	0.1
C/S/H soluble coke (wt%)	–	89.0/8.0/3.6	89.2/7.5/3.0	89.5/7.2/2.8	89.3/7.1/3.0
$I_W/(I_{Al} + I_{Ti})$%	3.21	2.45	2.10	2.12	–
$I_{Ti}/(I_{Al} + I_{Ti})$%	7.8	5.9	5.1	5.4	–

bon and sulfur content were slightly increased. The differences in physical properties between Spent 1, 2 and 3 samples were relatively small, but noticeable. The analysis of spent catalyst obtained from the commercial unit showed 6.0% by weight of carbon, 6.2% of sulfur. Its physical properties are similar to those of Spent 3 catalyst. The pore size distribution analysis in all deactivated samples indicated that an important part of the microporous structure had been lost due to coke deposition, which is responsible for an initial-significant-reduction in activity. This observation reveals the relatively low-value of the activity and selectivity obtained with the one-week catalyst. A uniform coke deposition across the 1-mm particle diameter for all samples was observed using SEM-XR micro-diffraction analysis (but not shown here) that might indicate a similar deactivation mechanism occurring in both samples: pilot plant and commercial operation. The programmed thermal treatment of spent samples from 30 °C to 350 °C in argon shows 2%, 1.4%, 0.8% weight losses, respectively, for Spent 1, 2, and 3 catalysts, which indicates a progressive aging of the carbonaceous deposits that reduce the H/C ratio and increase the aromaticity of the carbonaceous deposit, a fact well established in the literature [24–26]. The commercial catalyst that had worked for a longer period of time lost only 0.5 wt% under argon treatment. Notice that all samples were extensively washed and dried at 200 °C before the argon treatment, and the spent catalysts do not contain the adsorbed xylene-soluble species.

The spent and commercial samples were treated with CH_2Cl_2 and the extract analyzed by GC–MS techniques (soluble coke). Fig. 1 shows the result of the analysis for Spent 3 and the commercial sample extracts. For example, the amount extracted is 180%, 90%, and 40% higher in the Spent 1, 2, and 3 than in the commercial sample (Table 1). The identification of most of the aromatics in the spectra indicated the presence of fluorantene, benzo(*a*)-antracene, pyrene, and benzo(*a*)pyrene that accounts for the 70% of the extract main components. Sahoo et al. [17] discussed the composition of the coke soluble in dichloro-methane for a CoMo hydrotreating catalyst, containing three

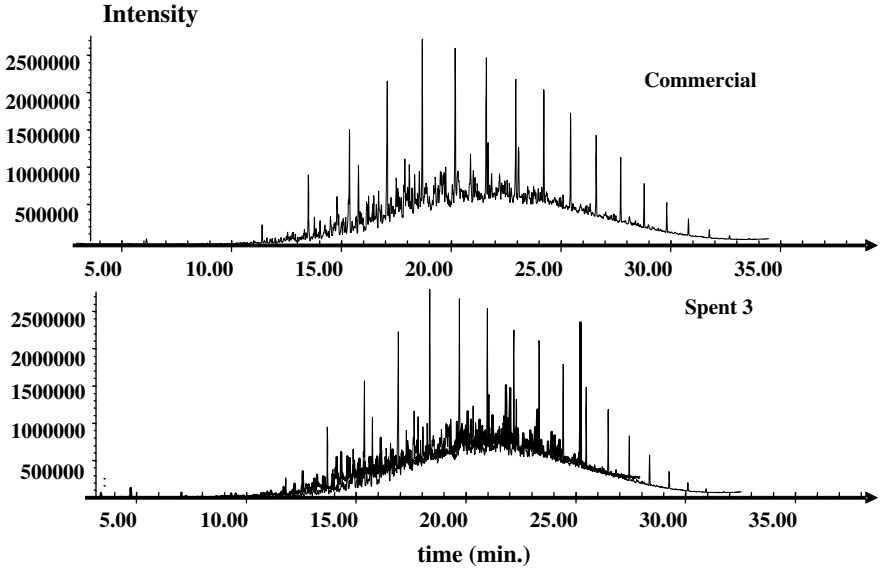

Fig. 1. MS analysis of soluble coke on (a) Spent 3 and (b) Commercial catalyst.

different amounts of zeolits in the support, that were deactivated in pilot plant (150 h on stream). They found a large difference in soluble coke between the deactivated catalysts that was attributed to the difference in feedstocks and zeolite content used by these authors. In our case, the composition of the extract does not match any of those used by them, and in addition it can be noticed that the soluble coke evolutes from Spent 1 to Spent 3 toward a more condensate type of compound, as it was expected. Thus the analysis of the soluble coke for the same feedstock depends upon the time on stream. But it is interesting to note that, even when there are small differences in the MS spectra of "soluble coke" between the commercial and Spent 3 catalyst, the fingerprint (products distribution) of the main compound are quite similar. These soluble carbonaceous materials are formed from 100% of LCO-feed in Spent 3 and from 15% of LCO in the feed used with commercial sample; thus LCO seems to play an important role in their composition. The carbonaceous materials are suspected of being the precursor of the insoluble coke which is formed by dehydrogenation and condensation of aromatics [24,26]. Some of these carbonaceous materials, though, had been split into volatile hydrocarbon and aged coke during the thermal treatment described above. The "insoluble coke" remaining in Spent 3 surface after dissolution of the inorganic matrix with HF, shows similar elemental composition than those obtained from commercial plant catalyst (see in Table 1 the C/H/S composition). It is important to note the presence of sulfur in "insoluble coke" that probably is formed through the condensation reaction from some of the most refractory poly-alkyl-sulfur-containing aromatics present in the reaction products. The chemical analysis of the "insoluble" coke does not show a significant presence of sulphided W, Ni or Pd that could contributed to the sulfur content in the coke.

Fig. 2 shows the solid ^{13}CNMR spectra for spent samples for the xylene-washed samples. The carbon deposit analysis allows us to understand the evolution of coke in the pores with time on stream and compare the commercial sample with those of the microplant. The upper spectrum corresponds to the commercial sample, and the intermediates to the Spent 2 and 3 samples. The 1-week sample (Spent 1) presents a well-defined peak at 135 ppm that is assigned to aromatics in polymeric structure [18,26,27]; other signals at 50 and 38 ppm that are attributed to aliphatic carbon structure. The spectrum of the 10-week sample shows one signal at 147 ppm and another at 115 ppm, the latter with a shift of 20 ppm with respect to the Spent 1 signal. The Spent 3 sample has lost virtually all the 50 and 38 ppm signals. These characteristics are in agreement with a progressive formation of a more organized turbostratic structure due to "aged" coke, and in agreement with the lower H/C ratio of the samples as a function of time on stream. Similar results were obtained by Callejas et al. [28] in hydrotreating catalysts used for residue upgrading. Note that the signals for the 10-week sample are quite similar to those observed in the commercial catalyst (upper two spectra in Fig. 1). The ^{13}CNMR analysis of the insoluble coke presents similar spectra for both mentioned catalyst with a main signal center in 147 ppm, results that differ than those obtained by Sahoo et al. [17], who founded a more insoluble "aliphatic" coke (30 ppm) in the hydrotreating (deactivated) catalysts.

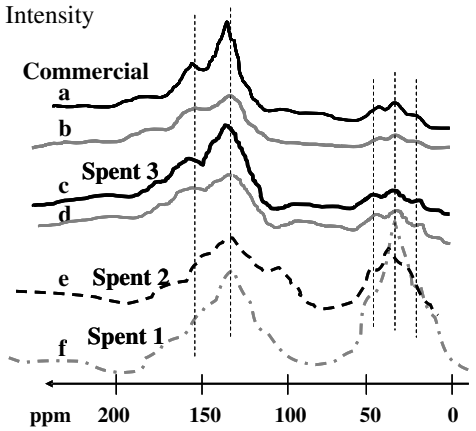

Fig. 2. ^{13}CNMR spectra of (a) commercial (b) insoluble coke on Commercial, (c) Spent 3, (d) insoluble coke on Spent 3, (e) Spent 2 and (f) Spent 1 catalysts.

Despite differences in catalyst composition and structure, the Spent 3 and commercial catalysts seem to have accumulated similar types and amounts of insoluble coke. Comparing this sample with other spent hydrotreating catalysts, operating without LCO and at different operating conditions, indicates that soluble coke deposits (end of cycle samples) have a quite different structure, but the insoluble coke was always of the same aromatic-type. The xylene-soluble species are dependant on feedstocks used, the reactor shutdown and catalyst downloading procedures, thus its analysis is disregarded here.

To understand the effect of coke on active phases, the metal dispersion was analyzed by XPS. The signals of W^{+4} ($W4f_{7/2}$: position 32.3 eV; FWHM: 2.05 eV) and Ni^{+2} (Ni $2p_{3/2}$: position 853.2 eV, FWHM: 2.1 eV) indicated that neither species BE were significantly modified by coke content. However, analysis of W dispersion on catalytic surface (see $I_W/(I_{Al}+I_{Ti})$ ratio in Table 1) indicated a 30% loss of metal concentration on the surface after 1 week on stream. At that point, the dispersion was slightly reduced by the additional time on stream. (Compare the ratios for Spent 1, 2, and three catalyst samples in Table 1). Similar reductions were observed for $I_{Ni}/(I_{Al}+I_{Ti})$ ratios. The $I_{Ti}/(I_{Ti}+I_{Al})$ signal ratio also decreased by 5.2% during the deactivation period, and it is observed that the broad Ti (2p) signal (two peaks: 456.7 and 459.1 eV) shows a shift in energy (down) of 1.2 eV, attributed to a change in the Ti–O–Al environment and characteristic of a spinels-type signal of Ti(IV) [29]. The $I_{Al}/(I_{Al}+I_{Ti})$ ratio varied in 6% without any particular shift in energy. A small (qualitative) difference in the FWHM was observed in the carbon signal for Spent 1 respect to Spent 3 samples that

was attributed to the presence of more aged deposit in the latter sample. Oxygen XPS signals were not modified along the time on stream; Sulfur in fresh catalyst showed just one signal (161.9 eV; FWHM: 1.88) attributed to $NiWS_x$ phase [30]. The spent catalyst presents two sulfur signals at 160.9 and 161.9 eV), the first one a small shoulder attributed to the S^{2-} in a carbonaceous environment, and another to the $NiWS_x$ phase. The presence of the signal at 160.9 eV indicated no oxidation in the sample during the transfer from the reactor to the XPS. The XPS dispersion measurements were verified using different angles for the beam; nevertheless, attenuations of metal signal by coke might be present. Changes (if any) in the weak palladium XPS signal (peaks at 336.2 eV due to Pd^{2+} and 335 eV to Pd^0) cannot be determined by this technique at this low concentration of metals. Nevertheless, a preliminary CO adsorption (FTIR) study showed a 30% reduction in Pd dispersion by catalyst deactivation [31]. All of this information indicated that surface carbonaceous deposits initially modified the metallic sites on the catalyst. These carbonaceous species-evolving as function of time on stream into a more aromatic-type of coke-fairly reduces the W and Ni dispersion, but does not change the type of sulfide species accessible to the XPS beams and their ratio. Some authors ([32], among others) postulated that the metal species migrated into the coke with a change in their sulfide state. We have no evidence of this migration, and for the purpose of interpretation the activity and selectivity results, it was assumed that the number of metal active sites might be decreased without changes in their intrinsic activities.

To investigate the effect of carbon deposition on acidity, a pyridine adsorption test was performed at 30 °C followed by thermal desorption at 200 °C and 300 °C. The fresh catalyst (Fig. 3a) showed the highest retention of pyridine of all samples because it had the cleanest surface exposed to the adsorption (negligible coke content). The spectra of pyridine adsorbed on this sample clearly reveal the presence of Brönsted (1548 and 1649 cm^{-1}) and strong Lewis (1633 and 1455 cm^{-1}) acid sites [33,34]. In addition, weak Lewis acid sites (1577 and 1488 cm^{-1}), as well H-bonded

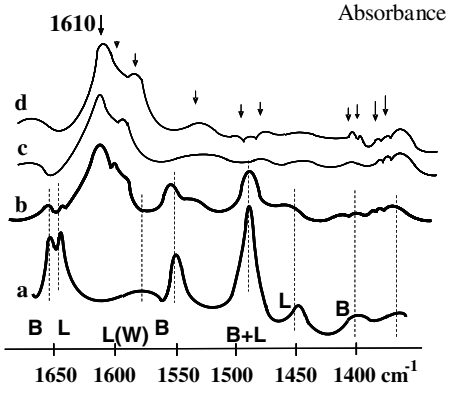

Fig. 3. Pyridine adsorption at room temperature on (a) fresh + pyridine, (b) Spent 3 + pyridine, (c) Commercial, and (d) Spent 3.

pyridine sites at 1390 cm^{-1}, were present in the fresh sample after argon treatment. The spectra of Spent 3 catalyst is depicted in Fig. 3d that shows the typical band at 1600–1610 cm^{-1} that is generally found to be proportional to the amount of coke [35]. This band is ascribed to highly unsaturated compounds such as polyolefins and poly-aromatics. This band slightly increases with the time on stream and is shifted toward lower wave numbers (from 1610 to 1603 cm^{-1}). Other bands at 1595, 1585, 1530, 1510, 1466, 1412, 1387, and 1368 cm^{-1} due to unidentified contribution aromatics polymers were observed in these and in previous samples of spent hydrotreated catalysts, and they are indicated with arrows in the Fig. 3d. Pyridine was then adsorbed on Spent 3; the spectrum is shown in Fig. 3b. By comparing the bands attributed to pyridine in fresh and Spent 3 catalysts, a dramatic reduction on acidity and a modification in the Brönsted/Lewis ratio can be observed. IR of Commercial sample is shown in Fig. 3c and the spectra is quite similar to Spent 3 sample (Fig. 3d), in agreement with thermal treatment results. The spectrum for Spent 3 and Commercial catalyst after extraction with dichloromethane (not shown) present only a small bands at 1603 cm^{-1}, but the other bands mentioned above had mainly disappeared [31]. The deconvolution of the IR spectra for fresh Spent 1, 2, and 3 provides the values of the Brönsted and Lewis sites as a function of time on stream. When the cycle progress, the adsorption of pyridine on Brönsted sites is more reduced than the Lewis type, and the Brönsted/Lewis ratio decreases as a function of time on stream (I_{1540}/I_{1450}: 2.1, 1.5, and 1.1 for Spent 1, 2 and 3 catalysts, respectively). This reduction in Brönsted sites is associated to the loss of Ti–O–Al-species that was observed by XPS at the beginning of the cycle. After then a continuous, but small, diminution of the Brönsted sites occurs, as well as of the Lewis sites as a function of time on stream.

The results of the total acidity measured by thermobalance for fresh Spent 1, 2, and 3 catalysts are reported in Table 1. After 1 week on stream, a dramatic drop in acidity (more than 60% in relation to fresh one) is observed. This occurred despite the help provided by the hydrogenating species (WNiPd clusters) and the presence of well-dispersed Pd that might be able to hydrogenate coke precursors. The early loss of acid site at the start of run is associated to an important reduction in volume and surface (microstructure) at the start of run where most of the coke is accumulated. At that point, the additional deposition of coke produces a small decrease in total acid sites. The ratio between the pyridine that remains adsorbed at 300 °C and that released by the catalyst in the 200–300 °C range gives an indication of the ratio between strong and weak acid sites (Table 1). This ratio decreases (2.5, 1.33, and 1) when the time on stream increases, indicating a relative lower survival of strong than weak sites. These results show a progressive reduction of the number and strength of acid sites accessible to pyridine, and an increase in Lewis/Brönsted ratio as a function of cycle length. The signal that

appeared at 980 cm^{-1} is attributed to pyridine adsorbed on Ti^{+4} species (Lewis-type sites) [36] that remained quasi constant in all spent catalysts. At this point the contribution of coke on the catalyst acidity is unknown, but activity test using insoluble coke and model molecules is in progress to check the point.

Finally, the effective diffusivity of pentane (200 °C, gas phase) indicates an important reduction in both macro- and micro-access in the spent catalysts as compared with the fresh one. Nevertheless, the difference in diffusivity between Spent 1, 2, and 3 samples is small (Table 1), indicating that the internal access to the structure is not progressively blocked by the additional coke deposition and their aging. Wood and Gladden [37] observed this blockage in commercial catalysts used in hydrotreating units with a variety of feeds. Thus, in our case, the effect of the cycle length, beyond the first week, on activity and selectivity (catalyst deactivation) may not be due to the small changes in internal diffusion of the reactant. Therefore, the deactivation needs to be related to the changes occurring on the active sites.

3.2. Microplant results

3.2.1. LCO product quality as a function of time on stream

Table 2 shows the properties of the products after operating for 1, 4, and 10 weeks on stream, indicated by Spent 1, 2, and 3 in the column end. The final temperature required to achieve around 50 ppm of sulfur in the products is indicated in the upper row. The catalyst performance shows a clear deactivating pattern and a higher temperature was needed as a function of time on stream to obtain the same sulfur in the product. Other sample of $WNiPd/TiO_2Al_2O_3$ catalyst had been previously operated with a straight run diesel, without LCO in the feed, and the temperature increase was only 5 °C for the same period of time and sulfur specification. Clearly the LCO is responsible for the fast deactivation of the catalyst, a well-known fact in commercial operation of middle distillated hydrotreaters.

It can be observed in the pilot plant results that changes occurred in the hydrogenation and cracking reaction balance as a function of time on stream. The relative rate of deactivation of the catalytic surface for the metallic and acid sites is responsible for the change in the aromatic ring hydrogenation and ring opening balance. This phenomenon had an impact in the yield and quality of the diesel produced during the cycle length. The results show that the hydrogenation capability was slightly lost, in spite of the increment in temperature performed, to compensate for the sulfur removal. Note in Table 2 that total aromatic hydrogenation (HDA) decreases from 68% to 50%. On the other hand, the amount of alkyl-benzene and alkyl-cyclohexane (products of the ring opening reactions) were reduced in greater proportion than the diaromatics conversion (hydrogenation) along the cycle length. As a result, an increment in mono-aromatics and naphthenic-aromatic content can be observed (rows 4th and 7th in Table 2) that result in a cetane number decrements from 44 to 38 (last row, Table 2). The same trend had been observed in commercial operation.

The conversion of aromatics rings into paraffins occurs through a complex network of reactions [38–40] that use both acid and metal sites. It starts by tri- and diaromatics ring adsorption on metal sites, where they are bounded by σ or π interactions (Fig. 4 upper part show an example for naphthalene hydrogenation). The hydrogenating reaction uses some hydrogen molecules adsorbed (σ bond) nearby in a metallic site (or by spillover in the border of clusters). The adsorbed alkyl-poly-aromatics can also suffer minor dealkylation (exocycle-cracking), losing its branches, as well as some hydrogenolysis of their side chains. The hydrogenated poly-alkyl-naphthenic-aromatics molecules

Table 2
Properties of the hydrotreated products as a function of time on stream (12.5 MPa, 0.2 h^{-1}, $4H_2$/HC)

Properties of the products	Feed	Spent 1	Spent 2	Spent 3
Temperature (°C)	–	350	364	378
Sulfur (ppm wt)	12,340	50	55	65
Nitrogen (ppm wt)	1230	30	45	55
Mono-aromatics (wt%)	15	12	15	17
Diaromatics (wt%)	35	10	15	16
Tri + Tetra-aromatics (wt%)	8	0	1	2
Mono-naphthenes (wt%)	5	18	20	21
Di-naphthenes (wt%)	10	12	14	16
Tri-naphthenes (wt%)	6	0	2	3
HDA (wt%)	0	68	55	50
Cetane number	<32	44	41	38

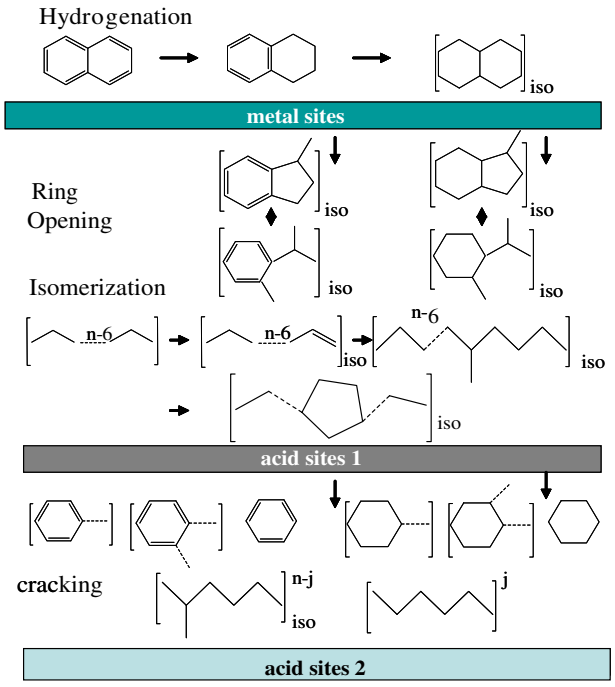

Fig. 4. Simplified scheme for hydrocracking of paraffins, hydrogenation of aromatics and ring opening of naphtho-aromatics.

desorbs from the metal site and migrate into the acid sites where the naphthenic ring might be protolytic dehydrogenated weak acid sites (Fig. 4 middle part). At weak acid sites, the naphthenic rings suffer then a skeletal isomerization to five rings, and immediately occur a ring opening via hydrogenolysis, or an endocycle cracking, to form another poly-alkyl-aromatic. Finally the alkycompounds desorbs from weak acid sites and absorb in the strong acid sites where they are cracked and dealkylated (lower part of Fig. 4). The cracking reactions reduce the "paraffinicity" of the products and their cetane number and change the aromatic distribution along the boiling range by transferring the heavy aromatics into the lighter part of the diesel. It is postulated, based upon current experiments with 1-pentyl-tetralin isomerization, that the tetralin and decalin are adsorbed on Lewis sites to form a five ring naphthenic intermediary that might desorbs or open into an alkyl-benzene molecule. Nevertheless other authors have proposed that the Brönsted sites are in charged of the isomerization [39–41]. There has also been much discussion about the role of the type of acid sites involved in the initial coke built up. No attempt is made here to clarify further the role of the Brönsted and Lewis acids until additional experiment might support the point. For that it is proposed that weak acid sites are used for isomerization and ring opening reactions, while strong acid sites are employed to crack the paraffins.

The exocycle-cracking of the alkyl (paraffinic branches) in aromatics and naphthenic molecules was verified by the analysis of the light (LD), medium (MD), and heavy (HD) cuts. It was found that the weight distribution, as well as the ratio of mono- to diaromatics (by weight), is changed along the cycle length (Table 3). Monoaromatics and mono-naphthenes that were concentrated in the heavier part at the beginning of cycle are shifted to the heavy part due to deactivation of the strong acid sites.

3.2.2. Test with synthetic feed

Table 4 presents the results obtained in the hydrotreating of a synthetic feed for the three deactivated samples of catalysts at constant sulfur removal activity. In presence of diaromatics, the dibenzothiophene (DBT) is mainly desulfurized into phenylbenzene (PB) using a direct route for sulfur removal, in agreement with previous results [11,19], in which the competitive effect of aromatic was demonstrated. The PB produced by desulfurization might be hydrogenated in competition with other aromatics and cracked to produce benzene. Detailed analysis of the product confirms the initial presence of 0.5% by weight of cyclohexylbenzene that decreases as the cycle progresses, due to the observed increasing amount of aromatics that may be adsorbed in the metal sites, thus reducing the DBT and PB hydrogenation rate of reaction.

Table 3
Mass and ratio for the LD/MD/HD fractions in Spent 1, 2, and 3 hydrotreated products

LD/MD/HD (wt%)	Spent 1	Spent 2	Spent 3
Mass	0.33/0.36/0.31	0.31/0.35/0.34	0.28/0.34/0.38
Mono/diaromatics	1.23/0.85/0.63	1.03/0.93/0.82	0.92/0.95/1.0
Mono/dinaphthenes	0.78/0.79/1.16	0.63/0.81/1.26	0.45/0.88/1.36

Table 4
Test of Spent catalysts by probe molecules (0.8 h^{-1}, 12.5 MPa, 4H_2/HC)

Composition/catalyst	Spent 1	Spent 2	Spent 3	Commercial
Temperature (°C)	340	348	356	363
Sulfur (DBT) (wt ppm)	50	53	49	52
Phenyl benzene (wt%)	1.4	1.8	2.0	2.3
Naphthalene (wt%)	2.7	4.9	8.8	7.7
Tetralin (wt%)	10.2	12.4	15.7	15.3
Methyl-indane (wt%)	0.8	0.6	0.5	0.1
Decalin (wt%)	9.0	11.8	13.0	15
Alkyl-benzene (all) (wt%)	10.2	6.1	3.1	1.2
Alkyl-cyclohexane (all) (wt%)	3.8	1.9	0.9	0
Benzene (wt%)	0.1	0.15	0.17	1.1

It can be seen in Table 4 that the start of run catalyst is able to produce a quite fast conversion of the naphthalene into tetralin and then into decalin. Tetralin was converted into methyl-indanes and then into alkyl-benzenes following a consecutive path of reaction. In the same way, decalin is transformed into methyl-bycliclo-nonanes and then into alkylcyclohexanes and others isomers (Fig. 4). All of these reactions reduce the concentration of tetralin and decalin and increase the cetane number by producing more "paraffinic" type molecules. Table 4, third and fourth columns, shows an increment in the intermediaries as a function on time on stream, in spite of the rise in temperature used to compensate the deactivation of the hydrodesulfurization. The fact that a small amount of benzene and a negligible amount of cyclohexane formed on spent catalyst products is due to the in-series effect on isomerization (deactivation of weak acid sites) and dealkylation (deactivation of strong acid sites). The amounts of ring-opened products (alkylbenzenes and alkylcyclohexanes) decreased and the amounts of dealkylated compounds (benzene and cyclohexane) increased with the time on stream. These factors indicated a reduction in the number of sites dedicated to ring opening and cracking, in agreement with the acidity measurement. Corma et al. [42] studied the cracking of tetralin and decalin on different zeolites as a way to characterize the LCO behavior and present the mechanism for the exocycle-cracking. This reaction is responsible of the molecular weight reduction of the alkylaromatics and the ring-opened molecules. In our case, the results of the tests done with the three catalysts at the same temperature (340 °C) have confirmed that the alkylbenzene/tetralin ratio is decreased by 15%, while that of benzene/tetralin is reduced by 30% as a function of time on stream. The changes in selectivity are due in part to the lower loss of weak than strong sites. Nevertheless, during the increase in temperature performed along the cycle length to achieve the 50 ppm of sulfur, the relative reaction rates on the weak

to those on strong acid sites are decreased due to the lower activation energy of isomerization than cracking and hydrogenation reactions [11,19,43].

At start of run, the *n*-C_{16} paraffin was 35 wt% converted into lighter *iso*- and *n*-paraffins, but after 10 weeks on stream, the cracking with Spent 3 catalysts was decreased to 25%, regardless of the rise in temperature from 340 °C to 356 °C. These reductions in cracking conversion confirm the reduction of the numbers of strong acid sites, in agreement with the pyridine measurement. The testing of the catalyst at the same temperature (340 °C) demonstrated that cracking reactions is 20% more reduced than isomerization that demonstrated the higher reduction on strong acid sites than on weak acid sites. Nevertheless, the higher activation energy of the cracking reaction than the isomerization ones produces at 356 °C higher ratio C_3–C_5 *n*-paraffins/C_5–C_{10} isomers than at 340 °C.

The analysis in detail of the paraffins generated by cracking of *n*–C_{16} is also important to understand the deactivation of both the weak and strong acid sites, since they provide information about the isomerization/cracking reactions rate that takes place during hydrotreatment of the synthetic feed. The carbenium ion mechanism using one acid site to explain the cracking of paraffins of was proposed 40 years ago [44–47], and was extended by Martens et al. [48] and by Froment [49] using single-event methodology. Fig. 4 that illustrates the simplified path of reaction based on carbenium ion rules, but extended to two acid sites mechanism [11,43]. The simplified scheme shows that the conversion of n and isoparaffins (C_{16}) starts by producing an olefinic or a cyclo-paraffin intermediary through a dehydrogenation reaction on metal or through a protolytic dehydrogenation on weak acid sites (middle part of Fig. 4). This conversion is followed by an in-series isomerization into nono-, di-, and tri-branched intermediaries (indicated in Fig. 4 by the bracket with the subscript i), which can desorb and be hydrogenated, or cracked and hydrogenated toward low-molecular-weight *n*-paraffins (j) and isoparaffins (p) (see lower part of Fig. 4).

Light paraffins (C_3–C_4) can be formed from synthetic feed by exocycle-cracking of the alkyl-benzene and alkyl-cyclohexane, as well as by cracking the *n*-C_{16}, but the C_7^+ paraffins are mainly produced from primary cracking of the C_{16} iso and *n*-paraffins. The ring opening reaction of a butyl-cyclohexane, for example, produced a negligible amount of C_7 and C_8 paraffin due to preferential cracking on theta carbon position [11,48]; the ring opening of cyclohexane (CH) might only produce C_6^- paraffins. Due to that the ratios of *iso*-/*n*-C_7 and *iso*-/*n*-C_8 paraffins are used here to measure the capacity of the acid sites to crack paraffins (primary cracking) and those of *ii*/*i*-C_7 to determine the ability to isomerizes paraffins.

Table 5 shows the C_7 and C_8 *iso*-/*n*-paraffin ratios in the Spent 1, 2, and 3 products, and the commercial catalyst. There is a similar decrease in the *iso*-/*n*-paraffin ratio (25%) and *n*-C_{16} cracking (26%) as a function of time on stream. However, the ratio of *ii*/*i*-C_7 ratio declines by 29%. The same tests done at 340 °C (not shown) for Spent 3 and Spent 1 catalyst indicates that the ratio *iso*-/*n*-C_7 paraffin decreases in 15% with the time on stream, while the cracking of *n*-C_{16} cracking is reduced in 45% and the *ii*/*i*-C_7 ratio in 22%. This results confirm the higher survival of weak than strong acid sites that might be due to the "protection" of the former ones by a nearby metal site (hydrogenation of coke precursor using Pd nano-dispersed) and to their lower participation in the coking built up than the second ones. Notice the progressive increment of the ratio of Lewis to Brönsted site content described above, that might support the idea of the role of Lewis acids in the isomerization of paraffins and naphthenes.

Table 5
Ratio *iso*/*n* C_7 and C_8 paraffins in the synthetic hydrotreated products[a]

Ratio wt	Spent 1	Spent 2	Spent 3	Commercial
Temperature (°C)	340	348	356	363
iC_7/*n*C_7 paraffin	1.6	1.32	1.21	0.90
iC_8/*n*-C_8 paraffin	1.8	1.55	1.35	1.04
ii/*i*-C_7 paraffin	1.4	1.10	1.00	0.6
n-C_{16} conversion (wt%)	35	28	25	14
C_3–C_5 (wt%)	2.4	2.6	2.8	3.5

[a] Obtained at the operating conditions shown in Table 2.

The *iso*/*n*-paraffin ratio, as well as the isomerization/cracking ratio, in the product obtained with the commercially deactivated catalyst is lower than that shown for the WNiPd catalyst. The fresh commercial catalyst (MoNi on alumina base) has a totally different ratio and strength of weak and strong acid sites (mainly Lewis type), and they might be deactivated differently due to the absence of noble metals to protect them. The low C_7 and C_8 isomerization capability at the end-of-run (Table 4) might explain the reduction in ring opening reaction and the cetane losses observed along the cycle length with commercial catalyst. It is worth noting, though, that commercial catalyst, at the operating conditions mentioned in Table 3 keep a high cracking (high yield on C_3–C_5) and dealkylation rates of reactions (see benzene production). The *i*/*n*-C_7 and *ii*/*i*-C_7 ratios are lower in commercial than in Spent 3 product, in agreement with the measured difference in total acidity and B/L ratio. The deactivated commercial catalyst also shows a much lower content in Lewis type sites than Spent 3 sample.

After the initial deactivation (first week in operation), the soluble coke produced by dehydrogenation-condensation of poly-aromatics and sulfur-containing poly-aromatics present in the LCO was converted little by little into soluble coke responsible for the additional losses of metal and acid sites. The creation of this soluble coke reduces the activity and selectivity as a function of time on stream.

3.3. Diesel engine test

To demonstrate the effect of deactivation on emission, the three hydrotreated LCO samples (Spent 1, 2, and 3)

were tested in stationary conditions using a Mercedes-Benz diesel engine. In parallel, the emissions were confirmed by averaging the values obtained by performing a EURO III driving cycle simulation (2000 rpm/350 kW/1364 kPa-break mean effective pressure). The stationary tests were done under standard conditions diesel engine testing conditions (Table 6), to compare the emission on particulates (PM) and nitrogen oxides (NO_x). Since the samples had different cetane numbers and compositions, the test shows the change in engine emission associated with both factors. The test shows that the lowest emission is produced by the SOR sample, the most hydrogenated product, with lower total aromatics and mono-ring-aromatics. The longer the time on stream, the higher are the NO_x and PM engine emissions (Table 6). This effect is attributed to combustion delay and the shape of the energy release. When fuel is injected into the chamber after the engine is cranked on, the liquid is atomized and the ignition begins. In this phase, called uncontrolled burning or flame propagation period, most of the PM precursors are formed by thermal cracking in which the volatile aromatics play an important role [50]. The second phase starts with full combustion, resulting in peaks of pressure and temperature. From that point on, most of the NO_x formed is associated with the maximum temperature attained. The pressure–volume curve for SOR product is flatter than those observed for the 4- and 10-week samples. That behavior is equivalent to an earlier (and better) vaporization and a lower maximum temperature for the SOR product than for the other samples. Table 6 shows that NO_x and PM increased as a function of time on stream. The measured SOR product contains a lower light aromatic component in the most volatile part of diesel, and due to that composition, achieves a better engine emission behavior. The commercial sample used as a reference has a higher emission for similar total aromatics content and cetane number but with a different of aromatic distribution. The effect of cetane and aromatics on emission is visible at this level of cetane number for a high naphthenic type diesel, and the emission results might be valid for all the vehicles 2002 and older ones. The blending of a deeply hydrotreated LCO at the end of cycle into a high-quality diesel pool would be in detriment of the engine emission performance, despite the resulting improvement in freezing point.

Table 6
Diesel engine emissions for hydrotreated products (EURO III)/2000 rpm/350 kW/1364 kPa BMEP, No EGR in use

Emissions	Spent 1[a]	Spent 2[a]	Spent 3[a]	Commercial[b]
NO_x (g/bhph)	6	9	17	12
PM (g/bhph)	0.1	0.4	1.1	0.7
Cetane number	45	43	41	42

[a] Blend 25% hydrotreated LCO with 75% hydrotreated SRGO (50 ppm S, 28% Ar).
[b] Commercial product.

4. Conclusion

The LCO contains a high percentage of aromatics and sulfur, and this fuel valorization is dependent upon conversion of the main component into paraffinic-type material boiling in the diesel range. The commercial catalyst is able to hydrogenate aromatics, but has very limited effectiveness in transforming them into paraffins. The commercial experiences using catalyst that produce low-sulfur diesel demonstrate a high deactivation as a function of time on stream when LCO is present in the feed. The hydrotreating study was performed using pure LCO and a particular $WNiPd/TiO_2Al_2O_3$ catalyst and the results indicate that

- Acid functions are deactivated faster than metallic function by coke deposition.
- Coke deposited on catalyst after 10 weeks on stream with 100% LCO looks similar in structure and composition than those observed in conventional last-generation HDT catalysts operating in a commercial plant with 15% of LCO in the feed. Both soluble and insoluble coke content poly-aromatics-sulfur compounds that seems to play a role in the coke built up.
- Catalyst's ability to open the ring in naphthenic molecules (alkyl-tetralin and alkyl-decalin) is continuously lost along the cycle length due to a slow deactivation of weak acid sites and to the low response to the reaction rate to the increase in temperature. The deactivation of strong acid sites progresses more quickly than those of weak acid sites but still contribute strongly to crack and dealkylate paraffins due to its relative important activation energy of this reaction respect to the ring opening reaction.
- The deactivation produces a decrease in cetane number and an increase of aromatics content that generated higher NO_x and PM emission in diesel engine operation.
- It seems that preserving the ring opening active center on catalyst from deactivation will be a critical issue in future LCO valorization to ultra-low-sulfur fuel.

Acknowledgements

The author would like to acknowledge the valuable contribution of experiments done by R. Alberti Tissano, and the support of the Simon Bolivar University (Caracas – Venezuela) and Texas A&M University (USA).

Appendix A. Supplementary data

Supplementary data associated with this article can be found, in the online version, at doi:10.1016/j.fuel.2008.01.025.

References

[1] Babich IV, Moulijn J. Fuel 2003;82:607.

[2] Galiasso Tailleur R. In: Diesel options to meet future US and European specification. Preprint of 6th world chemical engineering congress, Melbourne. Paper 13; 2001.
[3] Lee CK, Mc Govern S. PTQ 2001:35.
[4] Cooper BH, Donnis BBL. Appl Catal A: Gen 1996;137:203.
[5] Galiasso Tailleur R, Ravigli J. Appl Catal A: Gen 2005;282(1–2):227.
[6] Galiasso Tailleur R, Prada Silvy R. In: Effect of catalyst pretreatment in milhydrocracking operation. Preprint of AICHE spring meeting, New Orleans; 2003. p. 201.
[7] Galiasso Tailleur R. Fuel Process Technol 2006;87(9):759.
[8] Santana R, Do T, Santikunaporn P, Alvarez M, Taylor W, Sughrue JD, et al. Fuel 2006;85:643.
[9] Toppinen S. Liquid phase hydrogenation of some aromatic compounds. Doctoral thesis, department of chemical engineering, Abo Akademi university; 1996.
[10] Chowdhury R, Pedernera E, Reimert R. AIChE J 2002;48(1):126.
[11] Arroyo J, Galiasso Tailleur R. Kinetics model for n-C_{16} hydrocracking in presence of di-aromatics and DBT. Ind Eng Chem Prod RD, submitted for publication.
[12] Barbier J, Churin E, Marecot P. Bull Soc Chim Fr 1987;6:910.
[13] Martin N, Viniegra M, Lima E, Espinosa G. Ind Eng Chem Res 2004;43:1206.
[14] Villegas JL, Kumar N, Heikkila T, Lehto VP, Salmi T, Yu Murzin D. Chem Eng J 2006;120:83.
[15] Sahoo SK, Rao PVC, Rajeshwer D, Krishnamurthy KR, Singh ID. Appl Catal A: Gen 2003;244:311.
[16] Martinez MT, Jimenez JM, Callejas MA, Gomez FJ, Rial C, Carbo E. In: Froment GF, Delmon B, Grange P, editors. Hydrotreatment and hydrocracking of oil fraction. Elsevier; 1997. p. 311.
[17] Sahoo SK, Ray SS, Singh ID. Appl Catal A: Gen 2004;278:83.
[18] Gopal S, Smirniotis P. J Catal 2002;205(2):231.
[19] Galiasso Tailleur R. J Comput Chem Eng 2005;29(11–12):2404.
[20] Galiasso Tailleur R. In: Mass transfer in the pores deactivated by Coke. Preprint of the LACTYM Congress held in Caracas; 2004.
[21] Brigg D, Seah MP, editorsPractical surface analysis by Auger and X-ray spectroscopy. John Wiley; 1987. p. 511.
[22] EPA report. The effect of cetane number increase due to additive on NO_x emissions from heavy-duty highway engines. EPA420-R-03-002; 2003.
[23] De Brujin A. Trickle bed pilot plant testing. In: The 6th International congress on catalysis, London, paper B34; 1976. p. 121.
[24] Magnoux P, Cerqueira HS, Guisnet M. Appl Catal A: Gen 2002;235:93.
[25] Barbier J, Churin E, Marecot P. J Catal 1990;126:228.
[26] Robinson PR. In: Thermochemistry of catalyst deactivation ii: competition between hydrogenation, condensation and hydrocracking. Preprint 3c AICHE meeting, Houston, Tx; 2007.
[27] Bonardet JL, Barrage MC, Fraissard J. J Mol Catal A: Chem 1995;96:123.
[28] Callejas MA, Martinez MT, Blasco T, Sastre W. Coke ^{13}CNMR analysis. Appl Catal 2001;218:181.
[29] Ti Arillo MA, Lopez ML, Pico C, Veiga ML, Jiménez Lopez A, Rodriguez Castillon E. J Alloys Compd 2001;317–318:160.
[30] Zuo D, Vrinat M, Nie H, Mauge F, Shi Y, Lacroix M, et al. Catal Today 2004;93–95:751.
[31] Galiasso Tailleur R. In: Catalyst deactivation by aromatics during LCO upgrading to high quality diesel. Preprint European Congress in Chemical Engineering (ECCE-6), Copenhagen; 2007.
[32] Cerqueira HS, Ayrault P, Datka J, Magnoux P, Guisnet M. J Catal 2000;196:149.
[33] Eijsbourts S, van Leerman GC. B Soc Belges 1995;104(4–5):347.
[34] Corma A, Fornés V, Navarro MT, Perez-Pariente J. J Catal 1994;148:569.
[35] Meloni D, Martin P, Ayrault P, Guisnet M. Catal Lett 2001;71(3–4):213.
[36] Bonino F, Damin A, Bordita S, Lamberti C, Rechina A. Langmuir 2003;19:2155.
[37] Wood J, Gladden LF. Appl Catal A: Gen 2003;249:241.
[38] Rautanen PA, Lylykangas MS, Aittamaa JR, Krause AOI. Ind Eng Chem Res 2002;41:5966.
[39] Santikunaporn M, Herrera J, Jongpatiwut S, Resasco D, Alvarez W, Sughrue E. J Catal 2004;228:100.
[40] Kubicka D, Kumar N, Maki-Arvela P, Tiitta M, Niemi V, Karhu H, et al. J Catal 2004;227:313.
[41] Nylén U, Sassu L, Melis S, Järås S, Boutonnet M. Appl Catal A: Gen 2006;299(17):1.
[42] Corma A, González-Alfaro V, Orchillés AV. J Catal 2001;200(1):34.
[43] Galiasso Tailleur R. Fuel Process Technol 2006;87(9):759.
[44] Albertazzi S, Ganzerla R, Gobbi C, Lenarda M, Mandreoli M, Salatelli E, et al. J Catal 2004;228(1):100.
[45] Weitkamp J, Jacobs PA, Martens JA. Appl Catal 1983;8:123.
[46] Baltanas MA, Froment GF. Comput Chem Eng 1985;9(1):71.
[47] Poutsma ML. Mechanism considerations of hydrocarbons transformations catalyzed by zeolites. In: Rabo J, editor. Zeolite Chemistry and Catalysts, Washington, DC; 1976. p. 437.
[48] Martens GG, Marin BG, Martens JA, Jacobs PA, Baron G. J Catal 2000;195:253.
[49] Froment GF. Catal Rev 2005;47:83.
[50] Galiasso Tailleur R. In: Low emission diesel production in a mild-hydrocracker that use a gas phase reactor. Preprint world congress of chemical engineering, 7th, Glasgow, United Kingdom; 2005.